Analytica Chimica Acta, 161 (1984) 1—25
Elsevier Science Publishers B.V., Amsterdam — Printed in The Netherlands

INTEGRATED MICROCONDUITS FOR FLOW INJECTION ANALYSIS

JAROMIR RŮŽIČKA* and ELO H. HANSEN

Chemistry Department A, The Technical University of Denmark, Building 207, 2800 Lyngby (Denmark)

(Received 20th March 1984)

SUMMARY

A novel approach for constructing continuous flow systems for analysis is described and its versatility is demonstrated for a number of flow-injection systems with integrated potentiometric or optical detectors and with integrated gas-diffusion or ion-exchange units. Optimization of the miniaturized designs was achieved by means of scaling factors based on the theory of similarity.

The present work describes a departure from the traditional way of constructing flow-through systems for continuous flow analyses. Flow injection analysis (f.i.a.) [1] is used as an example to illustrate this novel approach and its versatility is demonstrated by means of several designs, which allow one to evaluate the new technology and its impact on the future construction of continuous flow systems. The idea, inspired by the concepts of integrated electronic circuitry, by discussions at the Gordon Conference in 1982, and by designs of gas chromatographs on silicone chips as originated at Stanford University [2], is based on miniaturization and integration of all components of a flow-through manifold into one unit, approximately of the size of a credit card. This means that instead of the individual manifold components (injection unit, mixing coils, dialysis or diffusion units and detectors) being joined by means of flexible tubing and connectors, the whole system of channels is fabricated into a planar surface of a plate, the plate being sufficiently thick to be mechanically stable and to accommodate optical flow cells, electrodes of electrochemical sensors, packed reactors, microcolumns, as well as inlets and outlets by means of which the integrated microconduits can be connected with external sources of liquids. The channels, imprinted or engraved in the planar surface, are sealed by another (thinner) plate, so that the cross-section of the channels is either semicircular or square. The thick and thin plates are bonded together and the resulting microconduits can even be stacked on top of each other to form a multilayered structure. Another attractive feature of this concept is that one or several detectors may be placed in the flow path exactly where desired, whereas in all previous constructions of flow-injection manifolds a compromise between the ideal and what was possible in practice was dictated by the physical size and geometry of the available flow-through detector.

0003-2670/84/$03.00

The development and construction of integrated microconduits was, however, a more complex task than might appear from the straightforward idea outlined above. Two groups of problems, conceptual and technological, were revealed as the work progressed, and although their solution is described separately below, it should be emphasized that it was the interplay of these two groups of problems which was the most difficult to solve, as material properties often imposed constraints on the intended design.

THEORY

Concepts of similarity

Any flow-injection system is built around a flow channel of certain dimensions and geometrical form (usually coiled tubing) and it would therefore seem to be an easy matter to miniaturize it by simply scaling down existing manifolds. The difficulty is that such an approach will not yield microchannels which would behave exactly like macrochannels, because a simple reduction of all dimensions does not produce channels which are physically similar. This may be better understood by briefly reviewing the concept of similarity as applied to fluid mechanics (e.g., [3]). The use of this concept for scaling and modelling of the behaviour of fluids is based on three types of similarities. The simplest, geometric similarity, is similarity of shape, and operates with a scaling factor which is the ratio of any length in one system to the corresponding length in the other system. Yet, when the channel for f.i.a. is miniaturized, perfect geometrical similarity will be impossible to obtain, because the roughness of the walls and other imperfections of the channels cannot be reduced proportionately when the overall dimensions are scaled down. Furthermore, an excessive reduction of the cross-sectional area of the channels is undesirable, because solid particles present in some sample materials (blood, fermentation liquids, etc.) could block a very narrow channel. Finally, since the idea was to imprint or to engrave a channel into a planar surface, rather than to wind a miniaturized coil, the concept of geometric similarity cannot be applied.

Kinematic similarity is similarity of motion and implies geometric similarity together with similar time intervals. Its scaling factors are velocities and accelerations. This would be a useful tool, if flow-injection systems of geometric similarity were available, because kinematic similarity would allow pumping rates to be adjusted. Dynamic similarity is a similarity of forces, which could also comprise a scaling factor; this type of similarity includes geometric and kinematic similarities, thus being a valuable tool for comparison of scaled models (e.g., for aircraft and ships). Outside the field of fluid mechanics, but still involving fluid properties, are thermal similarity which operates through differences in temperatures between model and prototype, and chemical similarity where the fixed ratios of reactants at corresponding points in the flowing streams serve as a scaling factor. Thus, in order for two systems to behave similarly, certain ratios of like magnitudes must be fixed.

Whatever quantities are chosen, the ratio of their magnitudes (i.e., the scaling factor) is dimensionless. Several scaling factors may be needed to describe a complex system like f.i.a., but once identified, they will allow a rational design and comparison of two flow-injection channels regardless of their geometric dissimilarity. To conclude, suitable scaling factors have to be identified and computed, as they will facilitate the design of miniaturized flow-injection systems which will behave similarly to the macrosystems (by yielding the same analytical readout) and yet will be more economical in terms of sample, reagents and space requirements.

Scaling factors

It is now widely recognized that flow injection analysis is based on the combination of three principles: sample injection of solution into an unsegmented carrier stream, controlled dispersion of the sample zone thus formed, and reproducible timing of the movement of the produced concentration gradient through the flow channel and detector.

A simple and practical method for designing a flow-injection system is based on the use of the dispersion coefficient $D = C^0/C$, where C^0 is the original sample concentration prior to injection and C is the concentration of the sample material in that element of fluid of the dispersed sample zone from which the analytical readout is to be obtained. As most f.i.a. methods are based on peak-height measurements, C is normally taken as the concentration of the dispersed sample solution in that element of fluid which corresponds to the peak maximum (C^{max}). The dispersion of sample solution is controllable by choice of sample volume and by geometry of flow and can be classified as limited dispersion (D = 1—3) if the system is to be used merely to transport samples reproducibly into the detector (e.g., for pH measurement); or as medium dispersion (D = 3—10), to provide a suitable mixing ratio between sample and reagent contained in the carrier stream (e.g., for spectrophotometry and chemiluminescence); or as large dispersion ($D > 10$), to be used when sample material has to be extensively diluted prior to measurement.

A response curve in f.i.a. is a result of two processes, the physical dispersion of the sample material in the carrier stream and the chemical reaction(s) forming the species to be measured, thus the dispersion coefficient D is a suitable scaling factor because it describes the ratio of reactants in that element of fluid which is chosen to yield the analytical readout. Because the physical dispersion and the chemical reaction are both kinetic in nature, and because they take place simultaneously, commencing at the same time (the moment of injection, S), they jointly yield a response curve, the time scale of which is the next scaling factor. As most methods in f.i.a. are based on peak-height measurements, the residence time, T, measured from the point of injection S to the peak maximum (Fig. 1), in conjunction with C^{max} allows (via D) the fixed ratios of reactants at corresponding times to be compared in geometrically dissimilar streams, thus yielding a basis for

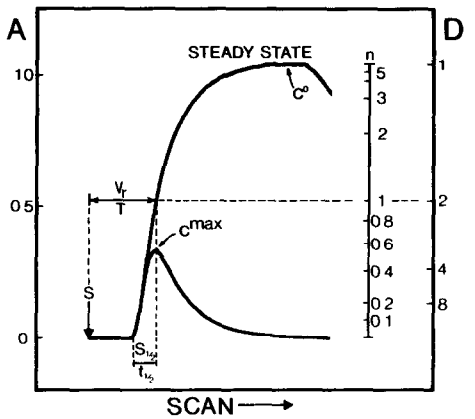

Fig. 1. The F curve and C curve obtained in a one-line flow-injection system (basic μ-conduit unit, cf. Fig. 3) by imposing a step and a pulse input, respectively, of a dye solution of concentration C^0 into an inert carrier stream, the signal being recorded as absorbance (A): S, point of injection; $S_{1/2}$ ($t_{1/2}$), sample volume (time) necessary to reach 50% of steady state; V_R, reactor volume; T, mean residence time; D, dispersion coefficient; n, sample volume expressed as number of $S_{1/2}$ values.

comparison of chemical similarity of otherwise dissimilar flow-injection systems. In other words, if a flow-injection procedure has been developed, optimized and tested in a macrochannel, it can be accommodated in a microchannel, provided that both systems yield similar D and T values. Going one step further, if D and T are identical for the micro- and macro-system, then both systems will yield identical readouts, which means that the same, say, spectrophotometric procedure will yield the same peak height (in terms of absorbance) provided that identical concentrations of sample and reagent materials are used in both systems, and that the flow cells have identical optical pathlengths and that the wavelength of the radiation to be absorbed is the same.

The last scaling factor to be identified must permit comparisons of economy of sample, reagent and time consumption in geometrically dissimilar flow-injection channels, as mere miniaturization of a system does not necessarily mean its optimization in terms of sampling frequency and consumption of liquid materials. In principle, one can use the D and T values for this purpose as well, for it has been shown [4] that

$$D = C^0/C^{max} = 2\pi^{3/2}r^2D_f^{1/2}T^{1/2}S_v^{-1} \quad (1)$$

where r is the tube radius, and S_v is the injected sample volume. If D_f (the axial dispersion coefficient) can be isolated, its value can be computed for a macrochannel and compared with the value computed for a microchannel. The system with lower D_f value would be more economical, as lower axial dispersion means less zone spreading. Because it has not been much appreciated (see, e.g., [5]) that the D value is related to the sampling frequency via

D_f (Eqn. 1), it may be more practical to use a more explicit term describing system performance. Such a term should allow estimation of: (a) the duration of the measuring cycle t_{cyc} (as t_{cyc} allows computation of sampling frequency); (b) peak width at the baseline Δt_b (as suggested by Vanderslice et al. [6]); and (c) sample and reagent consumption per measuring cycle. Such a term could also be useful as a more easily understood scaling factor than the axial dispersion coefficient D_f. To find it, Eqn. 1 can be rewritten as

$$D = C^0/C^{max} = 2V_r(\pi\delta)^{1/2}S_v^{-1} \quad (2)$$

where V_r is the volume of the flow-injection channel from the point of injection to the point of detection. Equation 2 assumes a Gaussian form of the peak because D_f is replaced by the dispersion number $\delta = \sigma^2/2$, σ being half of the peak width at 0.61 peak height, and $C^{max} = (4\pi\delta)^{-1/2}$. It has been established [1] that

$$1/D = 1 - \exp(-kS_v) = 1 - \exp(-0.693n) = 1 - 2^{-n} \quad (3)$$

where $n = S_v/S_{1/2}$, $S_{1/2}$ being the injected sample volume necessary to reach 50% of steady state; thus for $D = 2$, Eqn. 2 can be rewritten as

$$S_{1/2}/V_r = (\pi\delta)^{1/2} \quad (4)$$

The dispersion factor, $S_{1/2}/V_r$ can be obtained by a simple dispersion experiment simultaneously with the other two scaling factors D and T (see Fig. 1 and below). Because this factor is proportional to D_f and δ, the lower is its value, the less will be the axial spreading of the sample zone. Thus a flow channel with lower dispersion factor will operate with higher frequency and better economy of reagent and time than a system with a higher $S_{1/2}/V_r$ value.

The length of the measuring cycle (t_{cyc}), the peak width at the baseline (Δt_b), the carrier stream consumption (r_{cyc}), and the sampling frequency (S_f) are all functions of $S_{1/2}$ and V_r. For $S_v \leqslant S_{1/2}$, the values are given by

$$t_{cyc} = (V_r + 4S_{1/2})/Q \quad (5)$$

$$\Delta t_b = 4\,S_{1/2}/Q \text{ (or more conservatively } 6S_{1/2}/Q) \quad (6)$$

$$r_{cyc} = V_r + 4S_{1/2} \quad (7)$$

while $S_f = 60/t_{cyc}$ samples per hour for pumping rate Q expressed in volume units per minute. The maximum attainable sample frequency, S_{max}, will thus be given by $S_{max} = 60/t_b = 15Q/S_{1/2}$ samples/h.

The dispersion factor also allows all the above values to be predicted for longer or shorter sections of a flow channel of certain geometry. Because $S_{1/2}$ (Eqn. 4) is proportional to $\delta^{1/2}$ which in turn is proportional to the square root of the variance σ^2, and because the overall peak variance σ^2_{tot} is the sum of the variances contributed by the individual sections 1, 2, 3 . . . i of the flow path, i.e.,

$$\sigma^2_{tot} = \sigma_1^2 + \sigma_2^2 + \sigma_3^2 \ldots . \sigma_i^2 \quad (8)$$

and if the flow system is considered as a sum of N sections, each contributing the same $S^i_{1/2}$, then

$$S_{1/2} = N^{1/2} S^i_{1/2} \quad (9)$$

The dispersion factor is then obtained by dividing Eqn. 9 by the volume of the whole system, V_r

$$S_{1/2}/V_r = N^{1/2} S^i_{1/2}/V_r \quad (10)$$

If all sections are geometrically identical (i.e., each section contributes $S^i_{1/2}$), then $V_r = NV^i_r$, and

$$S_{1/2}/V_r = S^i_{1/2}/N^{1/2} V^i_r \quad (11)$$

Thus for a channel of uniform geometry, once $S_{1/2}$ has been established, it is possible to estimate the performance of a shorter or longer channel consisting of any number (N) of sections.

Straight channels or coiled tubing, or an imprinted channel of, say, sinusoidal form, or any channel of repeated geometry, may be viewed as consisting of a number of geometrically identical sections N. Because any deviation of geometry from a circular straight pipe will disturb the laminar pattern of the liquid flowing through the tube, the axial dispersion per reactor volume V_r will decrease from a straight pipe to a coiled pipe to a semicircular imprinted sinusoidal channel and will be smallest in a tube either packed with single beads (the SBSR reactor of Reijn et al. [7]) or three-dimensionally coiled (3-D coiled) [8] (cf. Table 1). The dispersion factor $S_{1/2}/V_r$ will decrease as the increased radial dispersion changes the character of the flow from mixed towards plug flow. Thus, once the scaling factors have been established for several types of channel, then the overall $S_{1/2}$ may be estimated for a system consisting of their combinations, by using Eqn. 10.

TABLE 1

Comparison of dispersion factors for five types of reactors of different geometry

Type of reactor	Cross-sectional reactor area (mm^2)	V_r (meas.) (μl)	$S_{1/2}$ (meas.) (μl)	Dispersion factor $S_{1/2}/V_r$
Microline[a]				
straight	0.2	172.9	70.6	0.41
coiled	0.2	193.7	66.4	0.34
3-D coiled	0.2	184.0	41.5	0.23
SBSR[b]	(0.6)	243.5	69.2	0.28
Basic μ-conduit unit	0.8	135.6	46.0	0.34

[a] 75 cm, 0.5 mm i.d. [b] Single bead string reactor (40 cm, 0.86 i.d.) filled with 0.5 mm glass beads; the effective cross-sectional area is different from the nominal one.

To summarize, the three scaling factors used here are the dispersion coefficient D, the residence time T and the dispersion factor $S_{1/2}/V_r$. The latter two can be obtained from a simple measurement, by injecting a large volume of a dye into a colourless stream and by recording the absorbance of the carrier stream with a flow-through colorimeter (Fig. 1). The step input, or F curve [1], thus obtained yields $V_r, S_{1/2}$ and C^0 (absorbance at steady state). Next, a sample volume of the size intended for use with the given flow-injection procedure is injected. This peak (C curve [1]) yields a D value, and a T value, and via Eqn. (3) reconfirms the $S_{1/2}$ value already obtained by the step input experiment. This in turn allows computation of t_{cyc}, r_{cyc}, etc. The D and T values are then compared with those of the macromethod and finally adjusted to match.

While the dispersion factor is determined mainly by the geometry of flow and to a lesser extent by the flow rate, D and T may be further manipulated by changing the injected sample volume (D), changing the flow rate (up to stopped flow) (T), and choosing the point of readout within the concentration gradient (D and T).

It is unnecessary here to reiterate the previously described gradient techniques [9], yet it is useful to illustrate how the D and T values can further be manipulated by a proper choice of the point of readout. So far, only the D and T values connected to the peak maximum have been discussed because most methods of f.i.a. are based on peak-height measurements at peak maximum. One may, however, choose any other element of the dispersed sample zone as a point of readout, if a finer adjustment of the D and T values is required. Thus two geometrically dissimilar flow-injection systems A and B may yield identical D and T values, as shown in Fig. 2. By injecting identical concentrations C^0 of a dye into these two channels, two response curves can be recorded from the same starting point (S). The peak-height measurement for

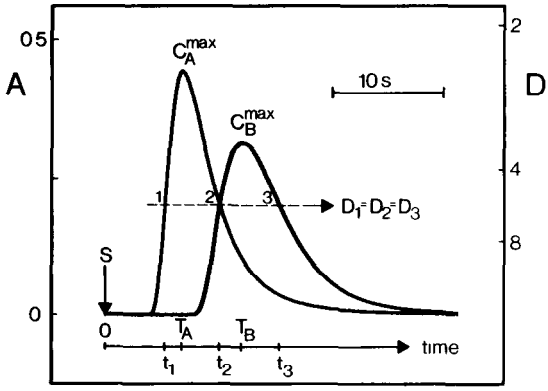

Fig. 2. Signal output for two dissimilar flow-injection systems where identical sample concentrations of a dye were injected, the responses being recorded from the same starting point (S). The two peak maxima, C_A^{max} and C_B^{max}, are related to the two residence times T_A and T_B, while times t_1, t_2 and t_3 correspond to fluid elements (1, 2, 3) with identical dispersion coefficients situated along the gradients of the dispersed sample zones.

channel A in this example has $D_A = C^0/C_A^{max} = 2.4$ and $T_A = 7.0$ s, whereas channel B has $D_B = C^0/C_B^{max} = 3.4$ and $T_B = 12.3$ s. These are the minimum D values obtainable in the given channel geometries, for the given sample volume injected. Higher D values can be obtained by fixing the readout at times other than those corresponding to the peak maximum. For illustration, points 1, 2 and 3 all have identical values ($D_1 = D_2 = D_3 = 5.2$), i.e., the same mixing ratio between sample and reagent (contained in the carrier stream). Point 2 also represents identical reaction times ($t_2 = 10.3$ s) for the two systems A and B, thus the readouts obtained at point 2 will be identical for both the A and B channels, regardless of how much these channels may differ geometrically. This observation has been exploited for evaluation of the selectivity of flow-injection methods [10] and will also be useful when the chemical scaling factor has to be adjusted for merging zones and instrumental pumping methods in macro- or micro-channels.

EXPERIMENTAL

Apparatus

All experiments were done with a Bifok-Tecator FIA-5020 Flow Injection Analyzer equipped with an injection valve of variable volume (Bifok, model L-100-1). For delivery and aspiration of liquids, both peristaltic pumps of the analyzer were used. The automated sequential operation of the pumps, and the timing of the valve functions, were controlled by the microprocessor of the FIA-5020. Optical measurements were made by means of a Bausch and Lomb Mini-20 spectrophotometer from which the light source (the tungsten lamp) was removed. The light from an external light source (20 W), powered by a variable power supply (4—8 V), was piped by an acrylic optical fibre (1.6 mm o.d.; Optronics, Cambridge, England) into the microconduit with integrated flow cell (see Figs. 6, 8 and 10) and from there by means of a second piece of optical fibre, the other end of which was placed where the tungsten lamp had originally been situated in the photometer. Both fibres were protected from ambient illumination by black PVC sleeving, and the cell compartment of the spectrophotometer was made light-tight. The transmittance signal from the spectrophotometer was fed to a logarithmic converter and then to the recorder (Radiometer Servograph REC-61, furnished with a REA-112 high-sensitivity interface), and from there to the FIA-5020. Results were displayed digitally on the FIA-5020 and also recorded on an attached printer (Alphacom, Sprinter 40). For potentiometric measurements, a digital pH meter (Radiometer PHM 64 Research pH meter) was used, the recorder being equipped with a REA-100 pH-meter interface (Radiometer).

Microconduits

All the microconduits for f.i.a. (Figs. 3, 4, 6, 8, 10, 12 and 13) were made from 70 × 45 × 10 mm transparent PVC blocks into which appropriate channel patterns were impressed or engraved. When closed by a transparent

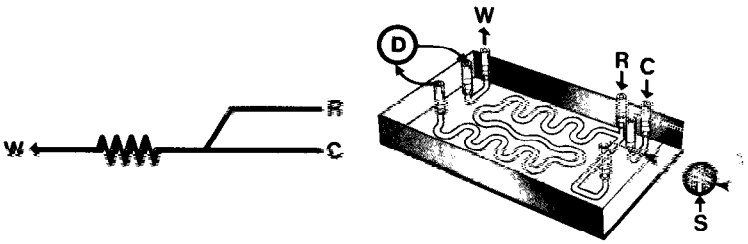

Fig. 3. Basic microconduit unit for f.i.a., designed to accommodate a carrier stream (C) to which a side stream (R) can be added in confluence, and to be attached to an externally placed injection valve (S) and detector (D). For the dispersion experiments shown in Fig. 1, the side stream R was not used. The channel length from the confluence point with R to the detector D is 15.6 cm.

plate with the aid of pressure-sensitive polymeric glue, the channels formed conduits of semicircular cross-section, typically with an area of 0.8 mm^2. Introduction of liquids into the channels and their withdrawal were effected through small perpendicular holes drilled at appropriate positions and furnished at the top with sleeving in order to facilitate connection to exterior tubing. Electrodes were implanted into the flow channels and milled flat so as not to protrude from the walls of the channel. In those microconduits where an optical flow cell was integrated, a 10-mm circular section of the transparent PVC block was replaced by a plug of black PVC of identical dimensions into which a hole serving as the flow cell (1.6 mm i.d., 10 mm optical path) was drilled perpendicularly to the conduit pattern. Covered on both sides with transparent plates, this construction ensured that only the light passing through the flow cell was transmitted to the acceptor light fibre (see Figs. 6, 8 and 10).

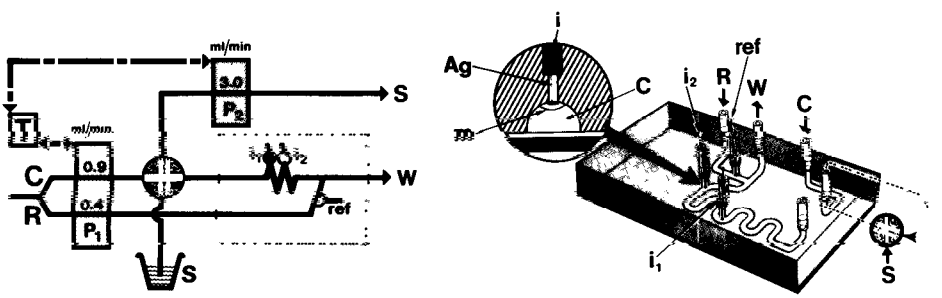

Fig. 4. Manifold and microconduit unit for potentiometric determination of pH, the components within the boxed area of the manifold being those contained in the microconduit. Pumps P_1 and P_2 are operated sequentially, controlled by timer T, so that sample (S_V = 30 μl) is first aspirated by P_2 into the injection valve (during which period P_1 is stopped) and subsequently propelled forward by carrier stream C (diluted buffer, c.f. Fig. 5) towards indicator electrode i_1 (or i_2), the construction details of which are shown in the inset (m is the pH-sensitive membrane). The reference electrode (ref) is placed in a side channel fed by stream R, and the combined streams are ultimately led to waste, W.

Electrodes

Silver wire (0.7 mm diameter) was implanted into the PVC block, and its surface, milled flush with the channel wall, was plated with silver chloride; this served as a reference electrode (cf. Fig. 4). The pH electrode was prepared as follows. First, a reference layer of $NaH_2PO_4/Na_2HPO_4/KCl$ was applied to the Ag/AgCl surface and then a pH-sensitive PVC-based membrane containing tri-n-dodecylamine [11] was cast over its surface. The casting procedure was repeated three times, and the membrane was then allowed to dry overnight. After the channel had been closed, the structure obtained was as shown in the inset of Fig. 4.

Reagents

All reagents were of analytical-reagent grade. Distilled and degassed water was used throughout.

For the dispersion experiments, the carrier stream used was 1×10^{-2} M sodium tetraborate to which was added 0.05% Brij. The bromothymol blue dye stock solution used for preparation of samples was made as described earlier [12]; a 1:200 dilution of this solution had an absorbance of 1.044 at 600 nm in a cell of 10-mm path length.

The carrier solution for the pH measurements consisted of 10^{-2} M sodium dihydrogenphosphate adjusted to pH 7.6 or 8.0, to which sodium chloride was added to give a final concentration of 0.10 M. This solution also served as reference solution for the Ag/AgCl reference electrode. Buffer standards in the pH range 2—12 were prepared as described in Tables 10.25, 10.37, 10.43, 10.45 and 10.5 in the monograph by Perrin and Dempsey [13].

The reagent carrier stream for the spectrophotometric determination of calcium was identical to that described previously [12], except that the alkaline solutions of diethylamine and *o*-cresolphthalein complexone, which in the earlier version were pumped separately into the flow-injection manifold, were here premixed in a container before being pumped. Calcium standards in the range 2.5—15 mg l^{-1} were prepared by dilutions of a 100 mg l^{-1} calcium stock solution [12].

RESULTS

Comparison of channels of different geometry, and design of basic microconduit unit

In order to verify the concept of the dispersion factor and use it for optimizing the geometry of the imprinted microconduit channels, $S_{1/2}/V_r$ values of various channel geometries were measured and compared by dispersion experiments. A step pulse of bromothymol blue in a colourless carrier stream of sodium tetraborate with ensuing colorimetric detection (*F* curve, Fig. 1) was used for this purpose. According to Eqn. 8, $\sigma^2_{tot} = \sigma^2_{inj} + \sigma^2_{reactor} + \sigma^2_{det}$, where $\sigma^2_{reactor} = \sigma^2_1 + \sigma^2_2 + \sigma^2_3 + \ldots$. Obviously, the dispersion factor will reflect the contributions from all these variables. Therefore,

the same injection and detector units were used in all experiments so that the contributions of these two components to the overall variance were kept constant. Furthermore, by keeping their volume minimal, σ^2_{inj} and σ^2_{det} were minimized. It should be realized, however, that because the total volume of the system, V_{tot}, is given by $V_{tot} = V_{inj} + V_{reactor} + V_{det}$, these non-reactor contributions, although constant, will become dominant when the reactor volume is very small. (Further, it should be noted that when the F curves are measured, i.e., the leading edge dispersion is recorded, σ^2_{inj} is independent of the injected volume, S_v, but reflects the volume, V_{inj}, of the connector between the valve rotor and the start of the investigated channel). Except for the SBSR reactor (which had an internal diameter of 0.86 mm and was packed with glass beads of 0.5 mm diameter) and the microconduits (imprinted into flat plates), all reactors were made of Microline tubing (70 cm, 0.5 mm i.d.) which was straight, coiled (coil diameter 10 mm) or 3-D coiled (by tying tight knots irregularly [8]). For coiled and 3-D coiled reactors, F curves were recorded as a function of reactor lengths L, starting with 100-cm long reactors, from which 25-cm sections were cut after each dispersion experiment (this was preferred to connecting shorter pieces of tubing, which could introduce changes in the flow pattern at the connecting points). The results of these experiments, summarized in Tables 1 and 2, show that the 3-D coiled reactor has the lowest dispersion factor (i.e., the lowest axial dispersion) and that this reactor (and the SBSR reactor) conform with Eqns. 8—11, because the radial dispersion promoted by secondary flow is sufficient, even in the shortest reactor length, to convert the flow-injection peak (C curve) to a near-Gaussian shape. In the coiled reactor, however, the secondary flow requires a longer length of line (L) to develop, and as σ^2_{inj} and σ^2_{det} become significant compared to $\sigma^2_{reactor}$ for 25 cm $< L <$ 100 cm, the development of the Gaussian shape of the C curves requires line lengths exceeding about 75 cm [1].

TABLE 2

Comparison of dispersion factors for Microline reactors (0.5 mm i.d.) coiled or three-dimensionally coiled, as a function of reactor lengths

Reactor type	Length (cm)	V_r (meas.) (μl)	$S_{1/2}$ (meas.) (μl)	Dispersion factor $S_{1/2}/V_r$	$(S_{1/2}/V_r)/(S_{1/2}/V_r)_{100}$	
					Measured	Theor.[a]
Coiled	25.5	85.7	31.8	0.37	1.08	1.98
	50	138.3	47.0	0.34	1.00	1.41
	74	192.0	66.2	0.34	1.00	1.16
	100	238.5	81.6	0.34	1.00	1.00
3-D coiled	25	85.7	27.7	0.32	1.79	2.00
	48	130.0	34.6	0.27	1.47	1.44
	71	179.0	38.7	0.22	1.20	1.19
	100	229.9	41.5	0.18	1.00	1.00

[a] According to Eqn. 11.

The microconduit (of 135-μl volume) has a dispersion factor of 0.34 which is similar to that of a 70-cm coiled tube (0.5-mm i.d.; 140-μl volume). Taking into account that the cross-sectional area of the coiled tubing is 0.2 mm^2 and that the microconduit channel is 0.8 mm^2, the geometry of the imprinted channel yields a lower axial dispersion than that of the coiled tube (cf. Eqn. 1). The basic microconduit unit (Fig. 3, where the basic unit is shown furnished with a second inlet, allowing addition of a side-stream R) is thus identical with a 70-cm coil of 0.5-mm i.d. tubing, in terms of sample, reagent consumption and time, provided that the same pumping rate Q is used. Conventional flow-injection systems are made of such coils (longer or shorter, as required), thus the basic unit may serve as a building block for those applications of f.i.a., which were designed originally for conventional systems with coiled tubing, because an appropriate choice of S_v and Q will yield identical or similar D and T values in microconduits and coils. For limited dispersion applications (such as pH measurements), a shorter channel has to be imprinted; for medium dispersion (e.g., methods for spectrophotometry or luminescence), one or two basic blocks are used, whereas for flow-injection titrations, the basic channel must be supplemented by a gradient tube.

Microconduit for pH measurement

As pH measurements require a system with low D value (1—3) and no chemical reaction is needed in the flow channel (thus allowing a short residence time T), a single line system with the lowest possible dispersion factor offers optimum economy of sample and carrier stream consumption per measuring cycle. Accordingly, the channel volume (between the point of injection and the indicator electrode i_1 in Fig. 4) was reduced to 20 μl, corresponding to $S_{1/2} \simeq 7$ μl, thus requiring $S_v = 30$ μl to reach $D = 1.05$. With $Q = 0.9$ ml min^{-1}, this yields theoretically $S_f = 60/t_{cyc} \approx 60\ Q/(V_r + 10\ S_{1/2})$ or a sample throughput of 600 h^{-1} (provided that the speed of response of the electrode is not the limiting factor).

The microconduit (Fig. 4) comprised the indicator electrode, i (two such electrodes, i_1 and i_2, are shown in Fig. 4 to indicate multisensor capability) and the Ag/AgCl wire reference electrode situated in a side channel and connected to the main channel downstream from the indicator electrodes. The manifold construction is such that the reference solution and thus the liquid junction are renewed during each sampling cycle when carrier stream is pumped (by pump P_1) through both channels. The construction of the pH electrode is described under Experimental. A typical pH readout, obtained by injecting buffers in the pH range 2.0—12.0 into a carrier stream consisting of phosphate buffer at pH 7.6 is shown in Fig. 5A; a recording obtained for the narrow pH range 7.0—7.8 (Fig. 5B, pH 8.0), corresponding to clinical applications, confirms the high reproducibility of this type of measurement (RSD 0.003 pH).

Because of the anion-exchange properties of the electroactive material

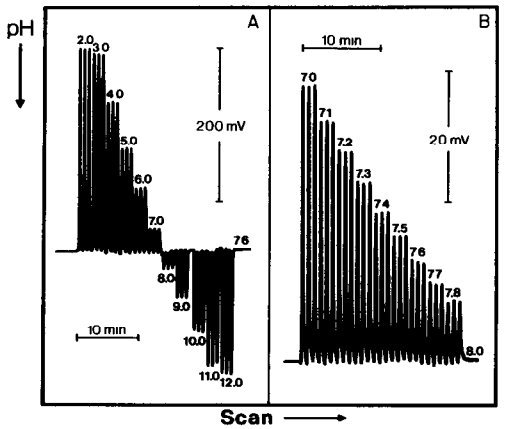

Fig. 5. pH-Response curves obtained with the microconduit system of Fig. 4. (A) A series of pH standards in the range 2.0—12.0; the carrier solution was a 0.01 M phosphate buffer containing 0.1 M NaCl, at pH 7.6. (B) Performance of the system in the physiologically important pH range; the carrier solution was at pH 8.0.

which is, like many other tertiary amines, capable of extracting anions into an organic phase (see, e.g., [14]), the electrode does not respond to pH changes below pH 3 in the presence of 0.1 M NaCl. The extraction of anions by tri-n-dodecylamine increases in the order $SO_4^{2-} < PO_4^{3-} < Cl^- < Br^- < I^- < ClO_4^-$, and it can be expected that the electrode selectivity will follow the same pattern, so that pH measurements would be unreliable even in neutral solutions in the presence of high concentrations of perchlorate. Above pH 10, interference is caused by alkali metal cations. In its present configuration, the sensitivity of the sensor towards chloride and alkali metal ions may give rise to a fine trough atop the peak if the dispersion is low and the pH is <3 or >9 in buffers without chloride, because the transition from the chloride-containing carrier stream to the chloride-free centre of the sample-buffer zone will affect the loading of the exchange sites on the electrode surface. Therefore, for more precise measurements, buffers should be used, containing chloride (and sodium ion) activities similar to those of the carrier stream. Despite these shortcomings, the electrode is very well suited to applications in f.i.a., as it has a fast response and low impedance, even when miniaturized. It is a useful device not only for direct pH measurement but also for indirect applications like pCO_2, ammonia and enzymatic measurements where the pH, generated on the other side of a gas-permeable membrane, reflects the concentration of analyte in the carrier stream (cf. Fig. 12). Its usefulness for blood gas measurements has already been confirmed [17].

In addition to the pH electrode, potassium-, calcium- and nitrate-selective PVC-based membranes have been applied in microconduits with success. Platinum and silver electrodes have also been tested for voltammetric and potentiometric applications.

Microconduit for spectrophotometry

Spectrophotometric measurements require medium dispersion of the sample zone within the carrier stream containing a colour-forming reagent. The basic unit, which has a volume of 135 μl and a dispersion factor of 0.34, yielded $D \approx 7$ with a sample volume of 10 μl. The determination of calcium, based on formation of the red-violet complex with *o*-cresolphthalein complexone, was used to test the performance of the microconduit with an integrated optical flow cell (Fig. 6). The reagents and sample concentrations were the same as described previously [12] and the manifold used was also similar (Fig. 6), except that the alkaline reagents of diethylamine and *o*-cresolphthalein complexone were premixed before use to avoid refractive effects (caused by the relatively high viscosity of the diethylamine reagent). To ensure sufficient supply of the reagents along the whole dispersed zone, a two-line system with a confluence point was used. The pumping rate Q was decreased to 0.75 ml min^{-1} in each line in order to achieve a residence time T of 6.5 s. Also, the sample volume was decreased to 10 μl in order to obtain a D value similar to the one used in the conventional flow-injection system for spectrophotometry of calcium. The resulting calibration curve (Fig. 7) is similar to that obtained with the macrosystem, but the sample

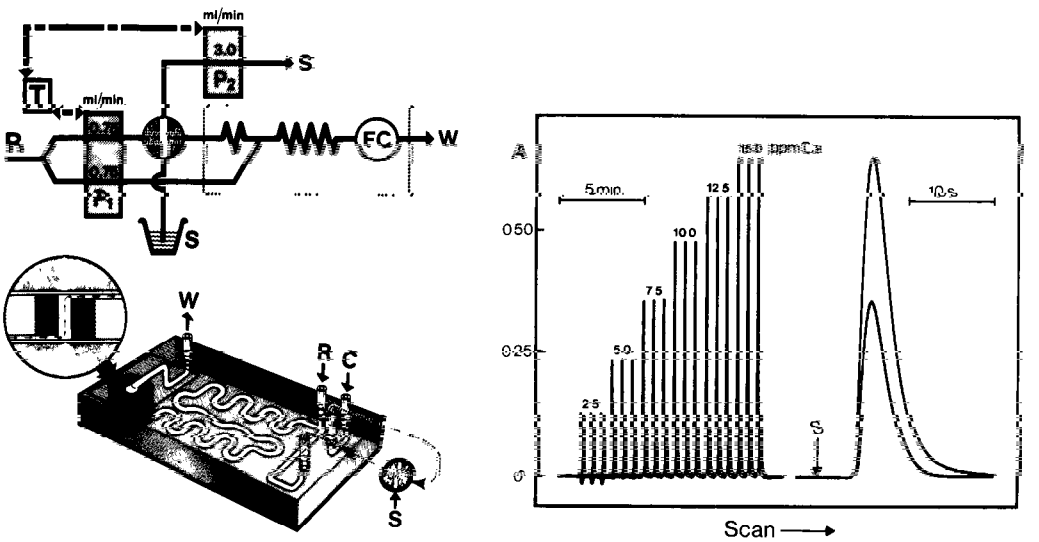

Fig. 6. Manifold and microconduit with integrated optical flow cell (FC), details of which are shown in the inset. Light is piped via optical fibres (see Fig. 10). The pumping rates indicated are for the determination of calcium (cf. Fig. 7) with this manifold.

Fig. 7. Response curves for the determination of calcium obtained with the microconduit system shown in Fig. 6 (S_V = 10 μl), where the reagent stream of alkaline *o*-cresolphthalein complexone was pumped to both inlets C and R, the stream being monitored at 580 nm. To the left is shown a series of standards in the range 2.5—15.0 mg l^{-1} Ca; to the right, standards containing 7.5 and 15.0 mg l^{-1} Ca are recorded at high chart speed.

and reagent consumption were reduced by about 50%. The dispersion factor for this flow channel is 0.34, thus the computed sampling frequency is S_f = 250 h^{-1}. The actual sampling frequency was lower because in automated operation additional time (in this case 11 s per cycle) is needed to fill the sample loop prior to injection, and this time interval must be added to each cycle. As there was no pressing need to operate at very high sampling rates, the cycle length was electronically selected in the Bifok/Tecator system to be 35 s, yielding a sampling rate of 103 h^{-1} (Fig. 7). As seen from the peaks recorded at high chart speed (Fig. 7), the sampling frequency could readily have been increased to the computed one (S_f) without carry-over. The flow cell functioned very well, though its windows became cloudy with use if any polymeric glue was left on the inside surfaces when the transparent plates were mounted. Thus, either both plates were replaced every two weeks, or the glue was carefully removed from the plates at the window areas before mounting. For u.v. measurements, thin quartz plates can be used instead of the thin plastic to cover the windows; the optical fibres connecting the light source to the flow cell and from the cell to the spectrophotometer must then also be made of quartz.

The experiments with the integrated optical flow cell have implications for fluorescence and chemiluminescence applications of f.i.a. The integration of potentiometric (pH) detectors and optical detectors on the same flow path will find many interesting applications.

Microconduit for high-speed titrations

Flow-injection titrations [4, 15] require medium to high dispersion, because it is not the peak height but the peak width which is the basis for the analytical readout. The theory of these titrations has been discussed [4, 15]. Essentially, the concentration C^0 of an analyte to be titrated is a function of the time span Δt between the two equivalence points situated on the rising and falling edges of the peak

$$\Delta t = (V_m/Q) \ln 10 \log [(S_v C^0)/(V_m C_{titr} n)]$$

where V_m is the volume of the mixing chamber, Q is the pumping rate, C_{titr} is the concentration of titrant pumped and n is the equivalent ratio of reacting species. Thus if phosphoric acid is injected into a carrier stream of sodium hydroxide, two equivalence points will be obtained (for n = 1 at pH 4.7, and for n = 2 at pH 9.6). It was shown previously [15] that a chamber with a mechanical stirrer can be replaced by a gradient tube (G) and the present design of the microconduit for fast flow-injection titrations reflects this feature (Fig. 8). For detection of the two equivalence points, by means of a spectrophotometer, a flow cell was integrated into the microconduit, and a mixture of the acid-base indicators, bromocresol green and thymol blue, which are both blue in the alkaline form and yellow in the acidic form, were added to the carrier stream of sodium hydroxide. Bromocresol green has its colour change in the pH range 3.8—5.4 and thymol blue

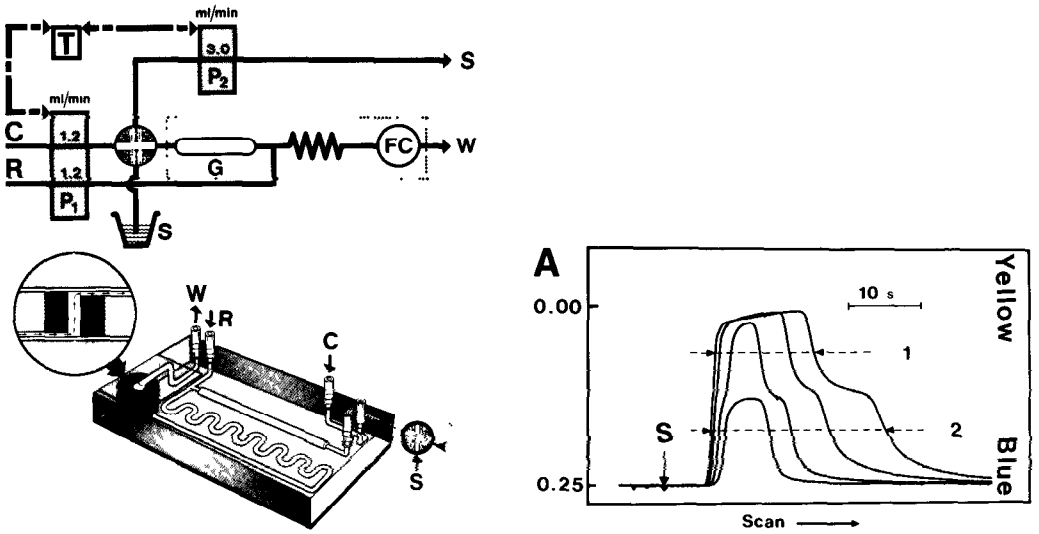

Fig. 8. Manifold and microconduit titration unit with integrated optical flow cell. After injection into carrier stream C (water) the sample is passed into the gradient chamber G and subsequently merged with the reagent stream R (NaOH + indicators), the combined streams being mixed in the coil before the flow cell.

Fig. 9. Titration of phosphoric acid with sodium hydroxide (1×10^{-3} M), using the microconduit system (and the pumping rates) described in Fig. 8 and an injected sample volume of 42 µl. See text for details. The titration curves are for $C^0_{H_3PO_4} = 2 \times 10^{-3}$, 4×10^{-3}, 1×10^{-2} and 2×10^{-2} M, respectively. The equivalence points are indicated by 1 and 2.

in the pH range 8.0—9.4, thus an abrupt change in the intensity of the blue indicators takes place when phosphoric acid is converted to $H_2PO_4^-$ and another change occurs on conversion to HPO_4^{2-}. The colour changes are detected by monitoring the absorbance of the carrier stream at 600 nm. The titration curves (Fig. 9) show the two equivalence points and the plateaux of least indicator change and maximum buffering capacities are visible on the leading and falling edges of the peaks, in analogy with classical titrations done batchwise.

Because the peak widths provide the analytical data for these titrations, the flow channel has to be designed to yield a large dispersion of the injected sample zone. This was achieved in the present design by incorporating a gradient chamber (G), 40 mm long, 2.1 mm wide and 1.8 mm deep (volume 138 µl); the D values at the two equivalence points 1 and 2 (Fig. 9) were then 7 and 21, respectively. Ideally, the volume of the gradient chamber should dominate the system because the concentration gradient would be purely exponential if the chamber were well stirred. But, for slower chemical reactions, sufficient reaction time would not then be allowed between the confluence point and the detector. This is why an additional length of channel was imprinted between the confluence point and flow cell; because

of radial dispersion within that section of the manifold, the exponential concentration gradient formed in G was partly transformed to a Gaussian shape. Consequently, Δt versus log C^0 did not yield a straight line over a very wide concentration range. A solution to this problem, together with results of flow-injection titrations based on redox, precipitation and complexiметric reactions, monitored by optical and electrochemical detectors, will be described separately [16].

Integrated microconduits

In all the above examples, the sample zone was injected into the microconduit channel from an external sampling valve, yet ultimately this function should also be integrated into the microconduit. Miniaturization of a rotary valve is one possibility, while another is the use of the hydrodynamic injection principle [9], which involves a combination of hydrodynamic and hydrostatic forces to aspirate, meter and inject the sample solution in the form of a well defined plug into the carrier stream.

To test this approach for sample injection and to demonstrate its flexibility, a manifold operated by two peristaltic pumps, controlled by timer T (Fig. 10), was constructed; two microconduits were used, the basic unit furnished with a flow cell, and the injection unit with an imprinted volumetric channel and two sample cups S_1 and S_2. The volumetric channel (17 μl) is shown in the manifold as the coil situated between points a and b, and is served by pump P_2. This channel forms part of two circuits; an open circuit starting in S_1 and leading through P_2 to S, and a closed circuit in which the inlets (R and C) and the outlet (to W) are hydrodynamically balanced so that the combined volumetric delivery of liquids to R and C equals the outflow to W. Thus when pump P_1 operates and P_2 does not, there is no movement of liquid between b and S_1 in either direction. The sampling cycle starts with P_1 in the stop position while P_2 is operating, as indicated by the solid lines in the upper corner of Fig. 11. During that delay period (DE1) the sample loop is washed and filled by sample solution from cup S_1. Next, pump P_2 is stopped and P_1 is activated, thus injecting the sample zone, located between a and b,

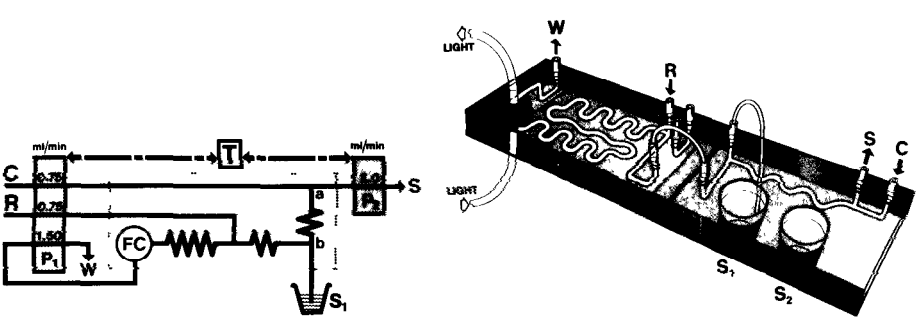

Fig. 10. Manifold and microconduit incorporating hydrodynamic injection and integrated optical flow cell. For details, see text.

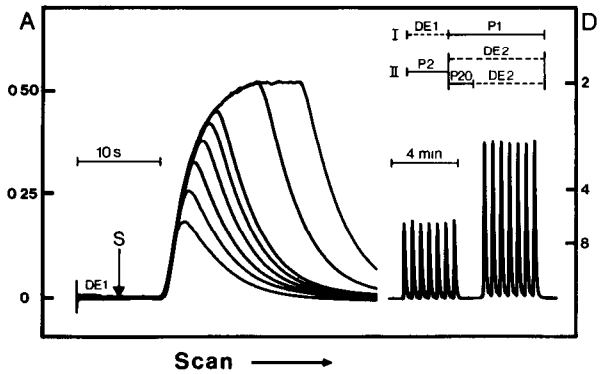

Fig. 11. Hydrodynamic injection of increasing sample volumes of a dye solution (bromothymol blue) into a carrier stream (1×10^{-2} M sodium tetraborate), using the manifold depicted in Fig. 10, monitoring the colour at 600 nm. To the left is shown a series of curves with increasing overlap times (P20) of the two pumps (0, 1, 2, 3, 4, 5, 10 and 15 s). Thus the smallest peak corresponds to an injected volume equal to the volume of conduit a—b in Fig. 10 (17 μl); for increasing overlap times, and so increasing S_v values, progressively higher peaks are recorded until the steady-state plateau is reached. To the right is shown the reproducibility of measurement for signals corresponding to P20 values of 0 and 3 s.

into the coil and through the analytical channel. By using a colourless carrier stream (1×10^{-2} M sodium tetraborate) and bromothymol blue as "sample" solution, the smallest peak shown in Fig. 11 was recorded. (The reproducibility of injection is demonstrated on the right-hand side of the figure, which shows the traces from repeated (7) injections of the same concentration of dye). In this mode of operation, the injected sample volume S_v corresponds exactly to the physical volume of the imprinted channel between a and b and therefore this approach may be termed as hydrostatic injection.

If the timing cycles of pumps P_1 and P_2 are allowed to overlap, the injected volume of sample can be increased at will. This can be understood by referring to Fig. 10 (left) and Fig. 11 (top right). In this mode, the cycle starts with a period during which P_1 is stopped (DE1) and P_2 is activated, filling the sample loop, but instead of the stop/go pattern being reversed after the DE1 period, both pumps are operated simultaneously for an overlap period (marked P20), during which pure sample solution is directed at point b towards the detector at a volumetric rate corresponding to that of the carrier stream C, while stream C itself is directed at point a towards S (along with an amount of sample corresponding to the volumetric pumping rate of pump 2 minus that corresponding to C). When pump 2 is stopped, carrier stream C is redirected through the sample loop and carries its content of sample towards the detector. Thus the amount of sample introduced is that aspirated directly during the overlap period, P20, plus the volume of the sample loop a to b; by increasing the overlap time, increasingly larger sample volumes can be injected, until the steady-state plateau is reached (Fig. 11). This is a true hydrodynamic injection as the sample zone is formed

by a combination of hydrostatic and hydrodynamic forces exerted on the columns of liquids by the two peristaltic pumps.

The reproducibility of the hydrodynamic injection (for an overlap time P20 of 3 s, corresponding to a total injected volume of 55 μl) is as good as that of the hydrostatic injection, as demonstrated by the second series of seven injections on the right-hand side of Fig. 11. In this connection, it is of interest that with the aid of hydrodynamic injection it is easy to measure all the experimental parameters discussed in connection with Fig. 1. Also, the curves recorded in Fig. 11 conform exactly with Eqn. 3, the only difference being that the steady state shown in Fig. 11 is now at $D = 2$. This is, of course, a natural consequence of adding a colourless stream R via the merging point to the injected sample zone in an exact proportion of 1:1 (0.75 ml min^{-1} + 0.75 ml min^{-1}); the original concentration of sample solution C^0 is halved and $D = 2$ is the minimum dispersion achievable.

It should be noted that the hydrostatically injected volume (S_v = 17 μl) and the sequentially increasing hydrodynamically injected volumes would not have conformed with Eqn. 3, if points a and b of the volumetric channel had been connected in the opposite manner, i.e., point a to the sample cup and point b to S, because sample material would then have been diluted by the carrier stream during the overlap interval P20 within the conduit a—b. This observation may serve as a warning as well as a hint to how various concentration gradients may be formed by means of the hydrodynamic injection principle. Finally, a drawback of both the hydrostatic and hydrodynamic injection methods should be mentioned: if the incoming and outgoing streams of the closed circuits are not perfectly balanced, then the sample solution in the cups S_1 will either be continuously aspirated (resulting in an increased and irregular baseline), or diluted by the carrier stream (thus yielding irreproducible result in repetitive sampling from the same cup S_1). Satisfactory balancing of the streams can be achieved by adjusting individually the tension of the pump tubes in the peristaltic pumps, because narrower, i.e., more elongated pump tubes, deliver liquids at lower rates.

Microconduit with diffusion unit

It is possible to laminate several layers of materials on top of each other and thus form channels which can be separated from each other within a selected section by a semipermeable membrane. Detail of such a structure is shown in the inset of Fig. 12: the flat channel for carrier stream C is separated by a gas diffusion membrane (d) from the acceptor channel (A) which is monitored by the above-described pH-sensitive electrode (i) with the treated PVC membrane (m), the Ag/AgCl reference electrode (r) being placed slightly downstream. Thus changes of pH caused by gas diffusing from the donor stream are easily monitored. The diffusion membrane has a very small area, usually 10 mm^2, and the diffusion time is very short because the dispersed sample zone passes through the diffusion unit in a matter of seconds. Thus the pH change in the acceptor stream would be too small if the acceptor

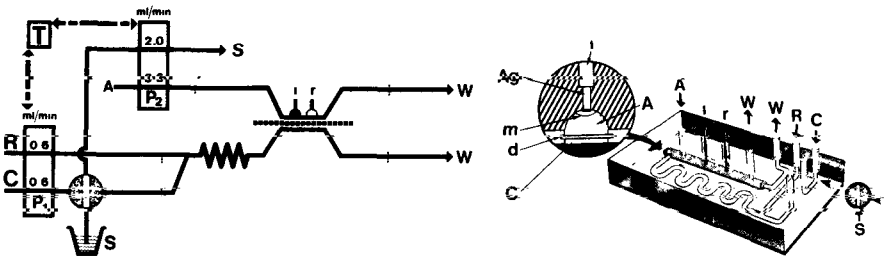

Fig. 12. Manifold and microconduit with integrated gas diffusion unit and potentiometric detection. The membrane (dashed line) separates two channels, containing the donor and acceptor streams, respectively. Any change in the composition of the acceptor stream is monitored by the electrode couple. The pumps are operated sequentially, controlled by timer T, and thus the acceptor solution is renewed after each measuring cycle. For details, see text.

solution were to move continuously during the measuring cycle. For this reason, carrier stream C and acceptor stream A are propelled by two different pumps (Fig. 12) so that when the carrier stream is in motion (P1), the acceptor stream stands still (P2). Thus, the diffusing gas material is concentrated in the vicinity of the electrodes, while the sample zone passes along the membrane. When the signal resulting from the pH change has been recorded, pump 2 is activated so that new sample solution is aspirated from the sample cup into the valve and fresh acceptor stream replaces the old solution around the electrodes.

This approach has been used successfully for measurements of CO_2 in blood [17] and, by analogy with conventional flow-injection systems [1], should be applicable to any diffusible species (e.g., CO_2, SO_2, NH_3). The use of an optical detector rather than electrodes may, however, require a more sophisticated flow cell of a smaller volume than the optical cell described above, should only a low concentration of a diffusible material be available. The reason is that a small volume behind a diffusion membrane of small area results in sufficiently high concentrations to be sensed by an electrode, but optical detection requires a certain optical path length, which can be obtained only by having a larger volume of a liquid than that surrounding the electrodes in the present construction.

Microconduit with an ion-exchange column

Previous work on preseparation of traces of heavy metals from sea water prior to atomic absorption spectrometry [18] demonstrated that a microcolumn filled with Chelex 100 (50—100 mesh) can be used to preconcentrate lead, cadmium and copper 20 times within a sampling cycle lasting 60—100 s. In this flow-injection system (Fig. 13), the column is first loaded by injecting 2 ml of sample by means of the valve and pump P1, and in the next cycle the metals are eluted with strong acid (E) by means of pump P2 which propels a zone of acid through the column and into the detector. Balancing of the

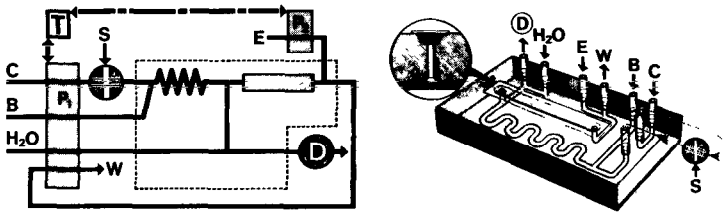

Fig. 13. Manifold and microconduit incorporating an ion-exchange column as used for preconcentration of metal ions [18]. The sample, injected into the carrier stream C, is mixed with buffer B to adjust the pH before entering the column. Metal ions are retained on the column and are eluted countercurrently by a small zone of eluent (E, acid) pumped by P_2. As the two pumps are operated sequentially, the eluted sample is carried to detector D (atomic absorption spectrometer).

streams and timing of the pumping cycles are in principle similar to those explained above for hydrodynamic injection; the nebulizer is supplied with wash solution (water) during the preconcentration cycle and the column is converted from the H^+-form to the NH_4^+-form after each elution sequence by means of buffer (B) which was also used to maintain and adjust the pH of the injected sample zone during the preconcentration cycle. Details of the procedure have been given [18]. The purpose of describing this approach here is to indicate the versatility of the microconduit concept, which allows incorporation of ion exchanging material into the flow channel. The groove filled with the ion exchanger (Fig. 13, inset), situated on the thicker plate on the opposite side of the channel system, allows renewal of the exchanger independently from the rest of the channel system.

Not only ion-exchanger columns of this type, but also columns filled with glass beads with enzyme attached to the surface are now being incorporated into microconduits. It is clear that many different combinations of detectors, diffusion units and enzyme reactors can be integrated into a unit of the size of a credit card. Such miniaturized flow systems can be manufactured reproducibly and, because of their small holdup volume, will serve well in economical serial analyses of discrete samples, or will become central components of continuous flow monitors for clinical and biotechnical applications.

DISCUSSION AND CONCLUSIONS

From a strict theoretical viewpoint, it might be objected that the assumption made in the derivation of Eqn. 11 is not justified because typical responses in f.i.a. are skewed and not Gaussian curves. This is why $S_{1/2}$ was assumed to be proportional (not equal) to σ, because increasing skewness of peaks obtained for short channels will cause increasing difference between σ and $S_{1/2}$. This can be seen from the results presented in the last two columns of Table 2 where nearly Gaussian peak shapes are obtained for the 3-D coiled reactors, whereas increasing skewness for decreasing coiled tube lengths causes increasing discrepancy between the measured and theoretical

values. A more detailed treatment of the limitations of Eqn. 1 has been presented [4]. However, the scaling factors suggested above are based on experimental values, accessible to direct measurements (V_r, $S_{1/2}$, Q, T, C^0, C), and can therefore be used for rapid and reliable estimation of characteristic properties and for mutual comparison of any flow-injection systems (S_{max}, t_{cyc}, S_v, N, n and D) without any reservations. Thus, existing methods of f.i.a. may be accommodated in channels of different dimensions and geometrical form by comparing the scaling factors, D, T and $S_{1/2}/V_r$, and by adjusting S_v and Q (and possibly the point of readout for gradient techniques) accordingly.

The dispersion factor, used here to optimize microconduit design, also allows macrochannels of different geometries to be compared, as illustrated by the results summarized in Table 1. Since Tijssen [19] suggested the use of tightly coiled tubes of narrow diameter (down to 10 μm), van den Berg et al. [20] proposed reactors packed with small particles and Reijn et al. [7] recommended the single bead string reactor (SBSR), it has become realized that each of these ingenious suggestions represents a compromise between what is ultimately desirable and what is practical, because high flow resistance, entrapment of air bubbles and danger of clogging the channels must be avoided. Given these practical limitations, and given the surprisingly low dispersion factor of the tightly knitted 3-D coiled flow channel suggested by Neue [8], the latter seems to be the best choice and therefore its features will be reflected in future designs of macro- as well as micro-conduits for f.i.a.

The concept of similarity has led to identification of scaling factors, which serve as practical guidelines for designing flow-injection systems. Similarly to D and T, $S_{1/2}/V_r$ describes all components of the particular system under investigation (i.e., the injection system, the flow channel, including sidestreams merging into it, and the detector). This is the strength, and weakness, of the present approach: it describes exactly the concentration ratios, residence times, sampling frequency and reagent consumption, but it is not precisely related to the variables strictly defined by the theory of flowing liquids (i.e., dispersion number δ, variance σ^2, and axial dispersion coefficient D_f). Several significant papers on flow theory have recently been published which use more rigorous approaches to the description of flow-injection systems. Thus the work of Reijn et al. [21] on optimization offers a valuable viewpoint, as does the work of van der Linden [22] on the theory of gas diffusion. The work of Pardue and Fields [23] also clarifies the interdependence of peak height and peak width relevant to the understanding of the dispersion process. A treatment of transport phenomena in f.i.a. without chemical reactions has been presented by Reijn et al. [24]. Recently, an instructive computer simulation, based upon the random walk model, was developed by Betteridge [25], describing the interplay of the dispersion process and the chemical reactions as they simultaneously occur in a f.i.a. system.

There is more than one way to describe the dispersion phenomena which occur during the movement of the sample zone towards the detector. They are all valuable, yet the choice of a general model describing the system satisfactorily is difficult because of the large variety of analytical problems to which f.i.a. is being applied. The theory describing a simple one-line system with a straight tubular channel designed for measurement of diffusion coefficients is straightforward, more complex flow-injection systems intended to handle sequential chemical reactions and separations have to be designed and optimized largely on empirical basis. The present approach, based on the use of D, T and $S_{1/2}/V_r$, is useful as a guideline for an initial design of a flow-injection system, and further optimization may be achieved by the conventional univariate optimization procedure or by computer-assisted modified simplex methods [26].

The examples of microconduit designs described above [27] amply illustrate the versatility of this new approach, which allows a wide range of combinations of basic components to be integrated into a compact unit. It is obvious that individual components, such as electrodes, optical flow cells, microcolumns with ion exchangers or immobilized enzymes, or gas-diffusion and dialysis units, may be combined and connected by channels of chosen geometry and length. These components can be placed exactly where required and not in a less favourable geometry as in conventional systems where the physical size and length of the connectors of the individual units dictate their minimum possible distance. By integration of all units, any connectors in the flow path through which the sample zones move are eliminated and so is the possibility of leaks and misconnections. Though certain skills and know-how are needed, it is relatively easy to make uniform microconduits. In the present version, a pressure-sensitive polymeric glue is used to bond the plates and to make laminated structures of layered channels, comprising all the required components including membranes. With this bonding technique, it is easy to reopen channels, remove individual layers, replace them, renew membranes, ion exchangers or immobilized enzymes, clean or renew electrode surfaces, replace optical windows in flow cells (should they have become translucent) or even to reroute those channels which have been cut within the sandwich of the bonded baseplates. This can be done quite quickly, if necessary under a microscope, with only a few tools; it is a matter of minutes to remove old layers and to replace them with new ones furnished with a fresh layer of glue. The price paid for this versatility is the low resistance of the materials used towards certain organic solvents, and swelling of the polymeric glue which causes blocking of channels if more concentrated acids (above 2 M) or alkalies are handled. So far, a wide variety of aqueous reagent solutions with additions of methanol, ethanol or diethylamine, has been used routinely for prolonged periods without any leak or blockage of the channels. Generally, it has been our experience that the microconduits are compatible with any solutions that PVC pump tubing can handle. The more aggressive solvents, such as chloro-

form, carbon tetrachloride, cyclohexanone, concentrated acids and alkalies, as well as higher temperatures (above 60° C), or pressures above the normal range for f.i.a. (>1 atm.), will require use of other materials and technology of bonding, such as photosensitive etching and bonding of glasses.

Further miniaturization of the microchannels by reducing the channel cross-section area (e.g., 4—10 times from the present area of 0.8 mm^2) would be easy even with the present technology and materials. However, the peripheral devices (pumps, injection valves, sample changers) are still relatively large so that there is not much point in making the integrated microconduits and their internal volumes smaller. The only commercially available instrument suitable for incorporation of microconduits (Bifok/Tecator FIA 5020) is about the size of an office typewriter, a size which, if further reduced, would motivate further reduction of the flow channels. Recent work on f.i.a. in the nanolitre range [28], with a flow channel built around a quartz capillary of 0.3 mm i.d., shows that further miniaturization is possible, provided that the channel geometry used allows operation at low pressure and reliable handling of liquids with particulate matter (such as blood). Future miniaturized flow-injection systems may operate with total volumes in the range of 10—100 μl per measuring cycle and sample volumes in the nanolitre range. The degree of scaling down will always be a matter of compromise between economy of sample and reagent and what is mechanically possible. If sample material is scarce and reagents are expensive (or toxic), or if multisensor units are required, the advantages of the miniaturized systems are obvious.

The authors express their appreciation to Jiri Janata, University of Utah, Salt Lake City, who, as an early participant in the construction of microconduits, has played a vital role in this project.

REFERENCES

1 J. Růžička and E. H. Hansen, Flow Injection Analysis, Wiley-Interscience, New York, 1981.
2 J. B. Angell, S. C. Terry and P. W. Barth, Sci. Am., 248 (1983) 36.
3 B. S. Massey, Mechanics of Fluids, 3rd edn., Van Nostrand Reinhold, New York, 1975.
4 A. U. Ramsing, J. Růžička and E. H. Hansen, Anal. Chim. Acta, 129 (1981) 1.
5 C. C. Painton and H. A. Mottola, Anal. Chim. Acta, 154 (1983) 1.
6 J. T. Vanderslice, K. K. Stewart, A. G. Rosenfeld and D. J. Higgs, Talanta, 28 (1981) 11.
7 J. M. Reijn, W. E. van der Linden and H. Poppe, Anal. Chim. Acta, 123 (1981) 229.
8 U. Neue, Chromatographia, 15 (1982) 403.
9 J. Růžička and E. H. Hansen, Anal. Chim. Acta, 145 (1983) 1.
10 E. H. Hansen, J. Růžička, F. J. Krug and E. A. G. Zagatto, Anal. Chim. Acta, 148 (1983) 111.
11 P. Schulthess, Y. Shijo, H. V. Pham, E. Pretsch, D. Amman and W. Simon, Anal. Chim. Acta, 131 (1981) 111.
12 J. Růžička, E. H. Hansen and A. U. Ramsing, Anal. Chim. Acta, 134 (1982) 55.
13 D. D. Perrin and B. Dempsey, Buffers for pH and Metal Ion Control, Chapman and Hall, London, 1974.

14 Y. Marcus and A. S. Kertes, Ion Exchange and Solvent Extraction of Metal Complexes, Wiley-Interscience, New York, 1969, Ch. 10.
15 J. Růžička, E. H. Hansen and H. Mosbæk, Anal. Chim. Acta, 92 (1977) 235.
16 T. G. Petersen, J. Růžička and E. H. Hansen, unpublished work.
17 L. Andisheh, N. J. Ho, J. Kratochvil, J. E. Moore, J. Růžička, L. Spritzer and B. Thompson, Int. Symp. Ion Select. Elect. Physiol. Med., Burg Rabenstein, Germany, Sept. 1983.
18 S. Olsen, L. C. R. Pessenda, J. Růžička and E. H. Hansen, Analyst (London), 108 (1983) 905.
19 R. Tijssen, Anal. Chim. Acta, 114 (1980) 71.
20 J. H. M. van den Berg, R. S. Deelder and H. G. M. Egberink, Anal. Chim. Acta, 114 (1980) 91.
21 J. M. Reijn, H. Poppe and W. E. van der Linden, Anal. Chim. Acta, 145 (1983) 59.
22 W. E. van der Linden, Anal. Chim. Acta, 155 (1983) 273.
23 H. L. Pardue and B. Fields, Anal. Chim. Acta, 124 (1981) 39, 65.
24 J. M. Reijn, W. E. van der Linden and H. Poppe, Anal. Chim. Acta, 126 (1981) 1.
25 D. Betteridge, private communication.
26 D. Betteridge, T. J. Sly, A. P. Wade and J. E. W. Tillman, Anal. Chem., 55 (1983) 1292.
27 J. Růžička, E. H. Hansen and J. Janata, Danish Patent Appl. No. 4296/82; U.S. Patent Appl. No. 478,227.
28 G. G. Vurek, 9th Int. Symp. Microchem. Tech., Amsterdam, The Netherlands, 1983 (Abstract No. VIII-21).